

# Formation and role of the interface region in ultrathin metal oxide layers for resistive gas sensors

Carlos Morales; Rudi Tschammer; Dominic Guttmann; Karsten Henkel; Jan Ingo Flege\* (Brandenburgische Technische Universität Cottbus-Senftenberg, FG Angewandte Physik und Halbleiterspektroskopie, 03046 Cottbus, Germany)

Carlos Alvarado; Christian Wenger (IHP – Leibniz-Institut für innovative Mikroelektronik, Im Technologiepark 25, 15236 Frankfurt (Oder), Germany)

\* [flege@b-tu.de](mailto:flege@b-tu.de)

## Abstract

In miniaturized gas resistive-sensor systems, understanding sensor performance and determining the optimal thickness of the active material requires an in-depth characterization of material deposition. In particular, the early stages of growth are mediated by interface formation and film/substrate interaction, which influence the mode of growth and the physico-chemical properties of the active deposit, likely affecting the sensor response for ultrathin layers. We present the use of *in-situ* X-ray photoelectron spectroscopy and *operando* spectroscopic ellipsometry for characterizing thin (<20 nm) atomic layer-deposited layers for use in next-generation miniaturized sensor devices. By targeting cerium and tin oxide layers, we demonstrate how these techniques can provide insights into their material composition, thickness, and optical properties during interface formation and the transition to bulk-like properties.

## 1 Introduction

The hydrogen economy proposes replacing current fossil fuels with H<sub>2</sub> produced from water splitting using electricity from renewable energy sources. However, the H<sub>2</sub>/air mixture is explosive at ambient pressure for concentrations between 4% and 75%. Therefore, to establish H<sub>2</sub> as a reliable and cost-effective fuel, we require safety elements such as H<sub>2</sub> detectors that can be easily integrated into mass devices.

Resistive sensors made from metal oxides have garnered significant attention due to their numerous advantages, including ease of thin-film nanopatterning, compatibility with integrated circuits, excellent performance with high sensitivity, and rapid response and recovery times. However, meeting market expectations remains challenging. This class of sensors requires either high-temperature heating for operation (>250 °C), which increases power consumption and compromises long-term stability, or the use of expensive noble metals, which raises manufacturing costs. As a result, current research is concentrating on two key areas: (i) creating new sensing materials that are highly responsive at low temperatures without expensive noble metal catalysts, and (ii) finding deposition methods that can create conformal, ultrathin layers on nanopatterned substrates with high effective surface area that can be easily integrated into CMOS technology.

In this context, atomic layer deposition (ALD) is a prominent technique in microelectronics, offering exceptional control over film thickness and conformality, including complex nanostructured surfaces, as well as precise growth of mixed compounds or heterostructures on demand. This is achieved by alternating pulses of organometallic precursors and oxidants, which can only react with the available surface sites in a self-limiting way. Moreover, the relatively low temperatures used for ALD growth, which are compatible with CMOS fabrication processes, yield defect-rich and nonstoichiometric thin films. Far from being a disadvantage, these intrinsic defects may induce modified

material properties compared to physical vapor deposited (PVD) counterparts and can even be beneficial in terms of increasing reactivity and thus sensor performance.

ALD processes are particularly suitable for growing ultrathin deposits, i.e., those with a thickness of a few tens of nanometers. However, such thin layers are critically influenced by the interaction with the substrate and the formation of complex interfaces, which likely affect the sensor response for ultrathin layers (< 5nm). Therefore, in miniaturized resistive-sensor systems, understanding sensor performance and establishing the minimum optimized thickness of the active material requires an in-depth characterization of material deposition, particularly at the early stages of growth. We present a combination of *in-situ* X-ray photoelectron spectroscopy (XPS) and *operando* spectroscopic ellipsometry for characterizing ultrathin (<20 nm) atomic layer-deposited layers of cerium and tin oxide (CeO<sub>x</sub> and SnO<sub>2</sub>, respectively). We demonstrate how these techniques can provide insights into composition, thickness, and optical properties of the deposited materials during interface formation.

## 2 Experimental methods

Our homemade ALD reactor consists of a stainless steel ultra-high vacuum compatible chamber with a base pressure of 10<sup>-8</sup> mbar, which is directly attached to the preparation chamber of the XPS system. The sample is positioned at the focal point of the chamber, below the entrance of the reactive gases, and its position can be precisely controlled through a 3-axis linear manipulator with a  $\theta$  rotator. The sample stage is capable of heating the sample to a maximum temperature of 1000 °C using a silicon nitride ceramic heater (343-HEATER SIN-8X10, Alletra). The temperature is monitored using a K-type thermocouple located near the sample and cross-checked against a temperature-dependent optical model for a Si(111) reference sample, as measured by ellipsometry, between 100 and 200 °C.

After the ALD growth, and once the pressure is below  $10^{-7}$  mbar in the ALD reactor, the sample is transferred to the XPS analysis chamber. More details can be found elsewhere [1].

The cerium oxide ( $\text{CeO}_x$ ,  $1.5 < x < 2.0$ ) layers were deposited using two different organometallic precursors by thermal ALD. First, by using the commercial precursor  $\text{Ce}(\text{thd})_4$  (Epivalance) in combination with ozone ( $\sim 7\%$ ,  $\text{O}_3/\text{O}_2$  mixture) generated with an ozone generator (OXP-30, Oxidation Technologies) and with a substrate temperature of  $250^\circ\text{C}$  [2]. Second, by using  $\text{Ce}(\text{dpdmg})_3$  - elaborated and provided by the group of Prof. Devi at Leibniz Institute for Solid State and Materials Research (Dresden, Germany) [3] - in combination with either  $\text{O}_3/\text{O}_2$ ,  $\text{O}_2$ , or  $\text{H}_2\text{O}$  at a substrate temperature of  $160^\circ\text{C}$ . The tin oxide ( $\text{SnO}_2$ ) was grown using the commercial precursor  $\text{TDMASn}$  (STREM) and  $\text{O}_3/\text{O}_2$ , at a substrate temperature of  $160^\circ\text{C}$ . In all cases, the ALD reactor was operated in flow-type mode using  $\text{N}_2$  as a carrier gas.

The growth of our ALD-active films has been systematically studied using *operando* spectroscopic ellipsometry (SER 801 UV-VIS, SENTECH) and *in situ* by X-ray photoelectron spectroscopy (XPS, Omicron EA 125) [1]. The inelastic peak shape analysis of XPS survey spectra was performed using QUASES software. The combination of these techniques comprises chemical and structural information of the ALD key actors (precursors, substrate, and film) during the early stages of growth, identifying key factors that can affect the sensing performance of ultrathin thin films such as changes in the growth per cycle (GPC), complex interface formation, and gradients in the oxidation state of reducible metal oxides.

### 3 ALD-based cerium oxide

#### 3.1 Hetero- and homodeposition regimes

The facile exchange between  $\text{Ce}^{3+}$  and  $\text{Ce}^{4+}$  oxidation states under reducing or oxidizing conditions makes  $\text{CeO}_x$  a promising candidate material for catalysis and sensor applications. For ALD films, the previously introduced intrinsic chemical and structural defects, along with film/substrate interactions, have been shown to critically affect their initial oxidation state [2] as well as their reducibility and sensing behavior towards  $\text{H}_2$  [4].

The deposition of ALD-based  $\text{CeO}_x$  using  $\text{Ce}(\text{thd})_4/\text{ozone}$  on  $\text{SiO}_2$  substrates illustrates the complex shift in the reaction mechanism that may happen as the precursor first interacts with the substrate and then with the deposit. This behavior defines two distinct growth stages easily differentiated by *in-situ* XPS characterization. During the initial heterodeposition regime ( $\text{CeO}_x$  directly grown on the substrate), the growth is dominated by non-ALD side reactions on the substrate, which, in the present case, result in greater GPC values and carbon residues, and prevent complete oxidation of the cerium oxide. In contrast, the steady homodeposition state stage ( $\text{CeO}_x$  grown on  $\text{CeO}_x$ ) is marked by a constant, literature-consistent GPC close to  $0.2 \text{ \AA}/\text{cycle}$ ,

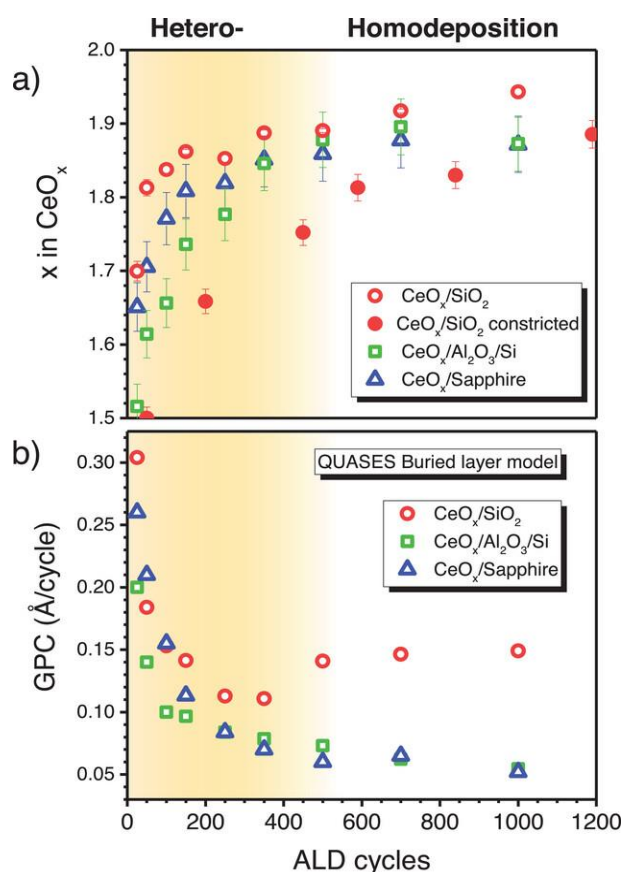


**Figure 1.** a) Stoichiometry of  $\text{CeO}_x$  deposits estimated from XPS Ce 3d spectra as a function of the total number of ALD cycles using  $\text{Ce}(\text{thd})_4/\text{O}_3$  (open red circles). The constricted exposure of Ce-precursor is shown by filled red circles. The stoichiometry of  $\text{CeO}_x$  deposits on ALD- $\text{Al}_2\text{O}_3$  on Si and c-sapphire is plotted in open green squares and blue triangles, respectively. b) Growth per cycle (GPC) values obtained from the inelastic peak shape analysis of XPS survey spectra in the Ce 3d region. Reproduced from [2], CC BY license from *Adv. Mater. Interfaces* published by Wiley-VCH GmbH

minimal carbon residues, and a fully oxidized cerium oxide film. These trends are not particular to  $\text{SiO}_2$  substrates and can be generalized to other metal oxide supports, such as c-sapphire and ALD- $\text{Al}_2\text{O}_3$  (10 nm) grown on Si wafers. **Figure 1** illustrates this shift in the growth mechanism, specifically the (**Fig. 1a**) average amount of  $\text{Ce}^{3+}$  states (i.e., reduced ceria) and the (**Fig. 1b**) GPC as a function of the number of ALD cycles.

The variation in the GPC can be used to explain the reaction mechanism by applying Puurunen's theoretical model [5], which relates the total amount of metal atoms attached per cycle with the size of the ligands (i.e., steric hindrance effect) and reactivity toward a specific surface (i.e., active sites available). During the homodeposition stage, a ligand exchange reaction is likely taking place: the density of Ce cations attached to the surface after a growth of  $0.2 \text{ \AA}/\text{cycle}$  ranges from  $0.45$  to  $0.50 \text{ nm}^{-2}$  for  $\text{CeO}_{1.5}$  and  $\text{CeO}_2$ , respectively, which are higher than the theoretical value assuming that no ligand release occurs ( $0.25 \text{ nm}^{-2}$ ). Moreover, the higher GPC during the heterodeposition regime cannot be

explained by the steric effect but is likely related to a higher density of initial active sites on the SiO<sub>2</sub> surface, which would promote non-ALD side reactions that increase the presence of carbon residues at the surface, as observed by XPS. Therefore, the initial stages of the growth are significantly affected by the substrate, which induces a change in the reaction mechanism.

More importantly for the chemical behaviour of CeO<sub>x</sub> as a sensor active layer, the Ce<sup>3+</sup> → Ce<sup>4+</sup> transition depends on three factors: (i) the easier reduction of ceria's surface compared to volume; (ii) the interaction with the substrate at the interface region; and (iii) the intrinsic ALD-defects. The first factor is intrinsically related to ceria regardless of the deposition process used. ALD can also enhance this effect by constraining the dose of Ce(thd)<sub>4</sub> during the corresponding pulse, thus preventing the complete coalescence of the cerium oxide islands, which now grow in clusters. As shown in **Figure 1a**, this situation leads to higher amounts of Ce<sup>3+</sup> states compared to the saturated growth. Secondly, the interaction with the substrate might be complex and will depend on the support. For Si-based substrates using PVD methods, it has been reported that the initial formation of silicates results in the stabilization of Ce<sup>3+</sup> states at the interface [6]. Here, by following the XPS Si 2s region plotted in **Figure 2**, we also observe the

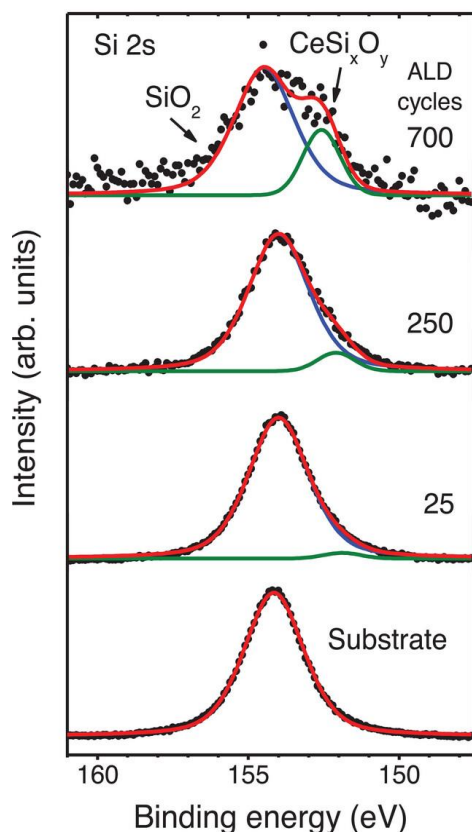


**Figure 2.** Si 2s XPS spectra as a function of the total number of ALD cycles for the growth of CeO<sub>x</sub> on SiO<sub>2</sub> substrates. The red line corresponds to the fit resulting from the Si 2s deconvolution into two components, SiO<sub>2</sub> (in blue) and CeSi<sub>x</sub>O<sub>y</sub> (green). Reproduced from [2], CC BY license from *Adv. Mater. Interfaces* published by Wiley-VCH GmbH.

formation of such silicates by the appearance of a second component shifted by 1.9 eV to lower binding energies than the SiO<sub>2</sub> line. It is worth noting that, in comparison with PVD processes, the Ce cations in the Ce(thd)<sub>4</sub> precursor already exist in the Ce<sup>4+</sup> oxidation state. Thus, their initial reduction under highly oxidizing conditions (O<sub>3</sub>/O<sub>2</sub> at mild temperatures) involves a complex chemical pathway, which is also reflected in the GPC values.

As for SiO<sub>2</sub>, the use of 10 nm thick ALD-Al<sub>2</sub>O<sub>3</sub> (on Si) as a substrate also results in the formation of aluminates at the interface. In this case, however, those Ce<sup>3+</sup> states are stabilized and cannot be further oxidized when submitted to a post-annealing process at moderate temperatures. These sorts of complementary measurements help establish a bottom-up approach for sensor design by primarily optimizing the active layer. Continuing with this example, the formation of aluminates hinders any gas sensor response when CeO<sub>x</sub> films are below 5 nm, thus excluding the use of ALD-Al<sub>2</sub>O<sub>3</sub> as the isolating layer between ceria and Si.

### 3.2 Role of ALD-intrinsic defects in sensing

The intrinsic ALD defects can be observed in two ways. First, by the incomplete oxidation of ceria layers under high oxidizing conditions, as observed for all substrates (the X-ray beam damage is small and can be discarded as a source of reduction). Second, by the lower crystallinity of ALD films. **Figure 3** shows *ex-situ* μ-Raman spectroscopy measurements for a 2.6 nm thick CeO<sub>x</sub> film on SiO<sub>2</sub> before (**Fig. 3a**) and after (**Fig. 3b**) a post-annealing process at 250 °C consisting of (1) sample reduction under H<sub>2</sub>, (2) subsequently back-oxidizing under an O<sub>2</sub> environment, and (3) final reduction again with H<sub>2</sub>. The change in the intensity of the F<sub>2g</sub> band at ~460 cm<sup>-1</sup>, in comparison to the Si signal (~300 cm<sup>-1</sup>), is a fingerprint of ceria crystallization, i.e., the healing of ALD-intrinsic defects, induced by post-annealing. While as-grown ultrathin films have been shown to promote H<sub>2</sub> heterolytic activation at room temperature and in the presence of diluted H<sub>2</sub>/O<sub>2</sub> atmospheres (H<sub>2</sub> concentration below 10%), recrystallization translates into lower reducibility, as confirmed by near-ambient pressure XPS measurements [4]. Therefore, ALD-intrinsic defects play a key role in ceria reactivity towards H<sub>2</sub>, replicating the expected sensing mechanism at low temperatures.

### 3.3 Tunable ALD-intrinsic defects

Similar results have been obtained when using the Ce(dpdmg)<sub>3</sub> precursor with three different oxidants (O<sub>3</sub>/O<sub>2</sub>, O<sub>2</sub>, and H<sub>2</sub>O) and substrates (Si, SiO<sub>2</sub>, and ALD-Al<sub>2</sub>O<sub>3</sub>/Si). While the same general trend regarding the Ce<sup>3+</sup>/Ce<sup>4+</sup> ratio is obtained for all growths and substrates as a function of the number of ALD cycles, the amount and variation of Ce<sup>3+</sup> states heavily depend on the chosen oxidizing species. Similarly, the amount and type of residues (carbon and nitrogen) depend on the oxidizing agent. For instance, and in line with density functional theory (DFT) calculations [3],

O<sub>2</sub> does not result in full oxidation but rather leaves Ce-O-N bonds, leading to the accumulation of nitrogen in ceria films compared to water or ozone.

Therefore, a careful selection of growth conditions allows for potentially tuning the intrinsic properties of ALD-based films via defect-engineering, including structural (i.e., low crystalline order, amorphous-polycrystalline deposits) and chemical (i.e., incorporation of light elements) defects.

## 4 ALD-based tin oxide

Lessons learned from the ALD-ceria deposits can now be applied and validated in the study of SnO<sub>x</sub> deposits. As determined by *operando* spectroscopic ellipsometry, the GPC is about 0.7 Å/cycle, as expected. In comparison to the ceria growth, no significant change in the GPC has been observed, indicating ideal linear film growth on Si for all cycles (see **Figure 4**). Meanwhile, XPS shows that the film is fully oxidized to SnO<sub>2</sub>. Interestingly, notable changes in the estimated Auger parameter during the early stages of growth indicate a shift in the chemical environment when the system transitions from the SnO<sub>2</sub>/SiO<sub>2</sub> interface to thicker SnO<sub>2</sub> films. At the same time, preliminary electrical measurements indicate a significant change in resistance and sensing behavior towards H<sub>2</sub> at low temperatures (100 °C) as a function of film thickness, which could be related

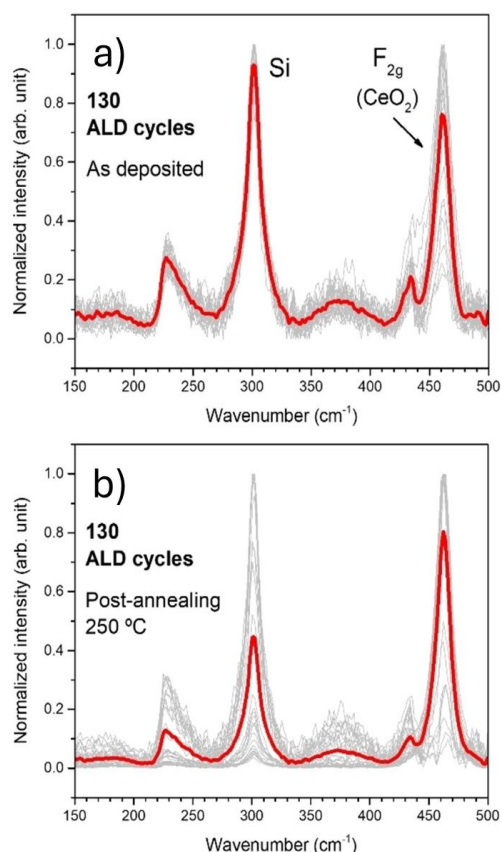


**Figure 3.** Raman spectra of as-deposited (a) 2.6 nm thick ALD-CeO<sub>x</sub> film (i.e. 130 cycles) and after post-annealing at 250 °C (b). The red spectra are the average of several individual spectra (light grey) taken at different positions. Reproduced from [4], CC BY license from *ChemSusChem* published by Wiley-VCH GmbH.

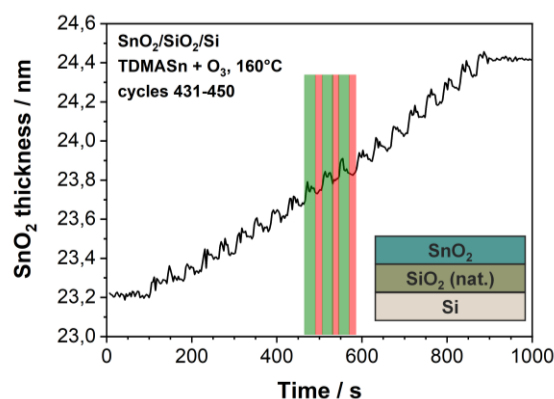


**Figure 4.** Ellipsometry data of ALD-SnO<sub>2</sub> growth at 160 °C using TDMASn and O<sub>3</sub>/O<sub>2</sub> on Si wafers. Green and red bars indicate the precursor and oxidant doses, respectively. Optical model shown in the right.

to either a change in the amount and type of chemical residues or the interaction with the substrate. Although further experiments are needed, the preliminary results suggest that the SnO<sub>2</sub>/SiO<sub>2</sub> interfacial region is a key factor in determining the sensing behavior of ultrathin SnO<sub>2</sub> films.

## 5 Conclusions

The intrinsic defects of the ALD deposit seem to play a crucial role in the physicochemical properties of ultrathin metal oxide layers. In combination with potentially strong film/substrate interactions, they can be used to tune the material's properties. This opens a new degree of freedom in active layers design while preserving the advantages of thickness and conformability control offered by ALD.

## 6 Literature

- [1] Morales, C.; et al.; Combination of Multiple *Operando* and In-Situ Characterization Techniques in a Single Cluster System for Atomic Layer Deposition: Unraveling the Early Stages of Growth of Ultrathin Al<sub>2</sub>O<sub>3</sub> Films on Metallic Ti Substrates, *Inorganics* 2023, 11, 477
- [2] Morales, C.; et al.: In situ X-ray photoelectron spectroscopy study of atomic layer deposited cerium oxide on SiO<sub>2</sub>: substrate influence on the reaction mechanism during the early stages of growth, *Adv. Mater. Interfaces* 2025, 12, 2400537
- [3] Kaur, P.; et al.: Rational development of guanidinate and amidinate based cerium and ytterbium complexes as atomic layer deposition precursors: synthesis, modeling, and application, *Chem. Eur. J.* 2021, 27, 4913
- [4] Morales, C.; et al.: Hydrogen sensing via heterolytic H<sub>2</sub> activation at room temperature by atomic layer deposited ceria, *ChemSusChem* 2025, 18, e202402342
- [5] Puurunen, R. L.: Growth Per Cycle in Atomic Layer Deposition: A Theoretical Model, *Chem. Vap. Depos.* 2003, 9, 249.
- [6] Allahgholi, A; et al.: Oxidation-state analysis of ceria by X-ray photoelectron spectroscopy, *ChemPhysChem* 2015, 16, 1083